[8] Y. T. Lo, D. Solomon and W. F. Richard, "Theory and experiment on microstrip antennas," *IEEE Trans. Antennas Propagat.*, vol. AP-27, No. 2, pp. 137–145, Mar. 1979.

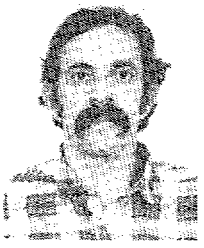

Sergio Barroso De Assis Fonseca (S'81) was born in Belo Horizonte, Brazil, on December 3, 1944. He received the B.S. degree with a gold medal in electrical engineering from the Polytechnic Institute of the Catholic University of Minas Gerais, Brazil, in 1971, and the M.S. degree in electrical engineering from the Catholic University of Rio de Janeiro, Brazil, in 1974.

From 1971 to 1972 he worked as an Engineer at Usinas Siderurgicas de Minas Gerais S.A.. He was a Teaching Assistant at the Catholic University of Rio de Janeiro in 1974 and an Assistant and Associate Professor at the Catholic University of Minas Gerais in 1975. Since 1976 he has been on the Teaching Staff of the University of Brasilia, Brazil, and is currently on leave, concluding his Ph.D. degree in electrical engineering at the State University of Campinas, Brazil. His primary interests are in the areas of electromagnetic wave propagation and antennas, with specific emphasis on microstrip antennas.

Mr. Fonseca is a member of the Brazilian Society of Microwaves (SBMO).

Attílio J. Giarola (M'58–SM'76) was born in Jundiaí, São Paulo, Brazil, on October 26, 1930. He received the B.S. degree in electrical and mechanical engineering from the University of São Paulo, Brazil, in 1954, and the M.S. and Ph.D. degrees in electrical engineering from the University of Washington, Seattle, in 1959 and 1963, respectively.

Before obtaining his Ph.D. degree he taught for several years at the Instituto Tecnológico de Aeronáutica, São José dos Campos, São Paulo, Brazil, at Seattle University and at the University of Washington. In 1962 he joined the staff of the Boeing Company, Seattle, and was responsible for research on infrared detectors and microwave devices. While on leave of absence from the Boeing Company, he spent two years in Brazil as an Associate Professor of Electrical Engineering at the Instituto Tecnológico de Aeronáutica and as a Visiting Professor at the University of São Paulo. During this time he was the Program Chairman of the First National Electronics Conference in Brazil and conducted research in solid-state devices. From 1968 through 1974 he was an Associate Professor of Electrical Engineering at Texas A&M University with the responsibilities of teaching and conducting research on electromagnetics, particularly on electromagnetic susceptibility. In 1975 he joined the State University of Campinas (UNICAMP), São Paulo, Brazil, where he has been responsible for the implantation and development of a research program in microwave devices. Since 1975 Dr. Giarola has been the Dean of the Graduate Studies at UNICAMP and from 1980 to 1982 he was the Vice-President of Academic Affairs of UNICAMP.

Dr. Giarola is a member of Eta Kappa Nu and Sigma Xi. He is a member of the executive committee of the Brazilian Society of Microwaves (SBMO).

Analysis of the Loop-Coupled Log-Periodic Dipole Array

JAMES M. TRANQUILLA, MEMBER, IEEE, AND KEITH G. BALMAIN, MEMBER, IEEE

Abstract—**A simple theoretical model is described to analyze the loop-coupled log-periodic dipole antenna (LPDA). Computed and experimental data are presented, comprising an investigation into both the far field and the dipole and feeder currents, for a wide range of antenna parameters. Particular attention is paid to a class of parasitic resonances characterized in the swept-frequency radiation pattern by a narrow-band reduction in front-to-back ratio. The calculations show that these resonances involve high out-of-phase currents in adjacent dipole elements, and also predict correctly their dependence on the nature and location of the feedline termination. Design data are presented showing how gain and front-to-back ratio can be optimized and parasitic resonance effects minimized.**

I. INTRODUCTION

THE LOOP-COUPLED log-periodic dipole antenna (LPDA) consists of an array of dipole elements sandwiched between two halves of a balanced transposed transmission line (Fig. 1) and separated from the transposed line by a dielectric clamp. The array is a backward-wave antenna with its feedpoint at the front (high frequency) end. Coupling of energy from the transmission line feeder to the dipoles occurs at those transpositions where the dipoles are approximately one half-wavelength long.

The loop-coupled LPDA has been studied experimentally [1] and has been optimized in the sense that anomalous frequency performance was minimized. However, no analytical treatment of the loop-coupled LPDA has been undertaken. Such an analysis is necessary to get design data over a wide range of parameters, and also to understand better the anomalous frequency performance and the methods for controlling it. Of particular importance is the determination of the relationship between the far field and the dipole and feeder current, which could confirm the supposition [1] that parasitic resonances on the feedline cause one type of anomalous performance, namely the high backlobe levels characteristic of overly loose coupling between the feeder and the dipoles. Also, much of the suggested explanation of the optimization procedure in [1] is dependent upon the dispersion characteristics of the transposed transmission line, but the effects of dipole loading on the dispersion curves were not calculated explicitly. Therefore, it is the purpose of this study to develop a simple analytical model for the loop-coupled LPDA and to validate the model experimentally.

II. CIRCUIT MODEL

Each cell of the loop-coupled array consists of a feedline section, a transposition section and a coupling region (Fig. 2(a)). For simplicity the coupling region is modeled at the center of

Manuscript received January 5, 1981; revised October 27, 1982. This work was supported by the Natural Sciences and Engineering Research Council under Grant A-4140 (University of Toronto) and Grant A-1068 (University of New Brunswick).

J. M. Tranquilla is with the Department of Electrical Engineering, University of New Brunswick, Fredericton, NB, Canada E3B 5A3.

K. G. Balmain is with the Department of Electrical Engineering, University of Toronto, Toronto, ON, Canada.

0018-926X/83/0300-0253$01.00 © 1983 IEEE

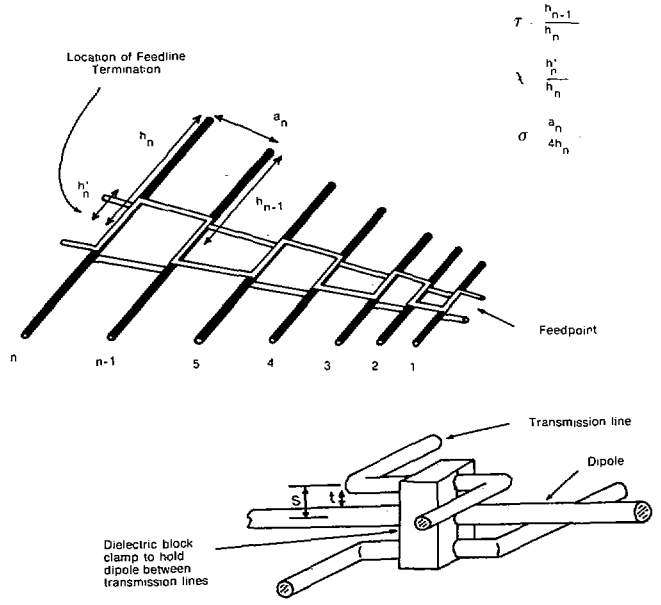

Fig. 1. The loop-coupled log-periodic dipole antenna showing details of element location between transposed transmission lines. All conductors are circular, 3 mm diameter. Note that t is the clearance separation between transmission line and dipole. The longest dipole is a free-space half-wavelength at 700 MHz, for all measurements and computations.

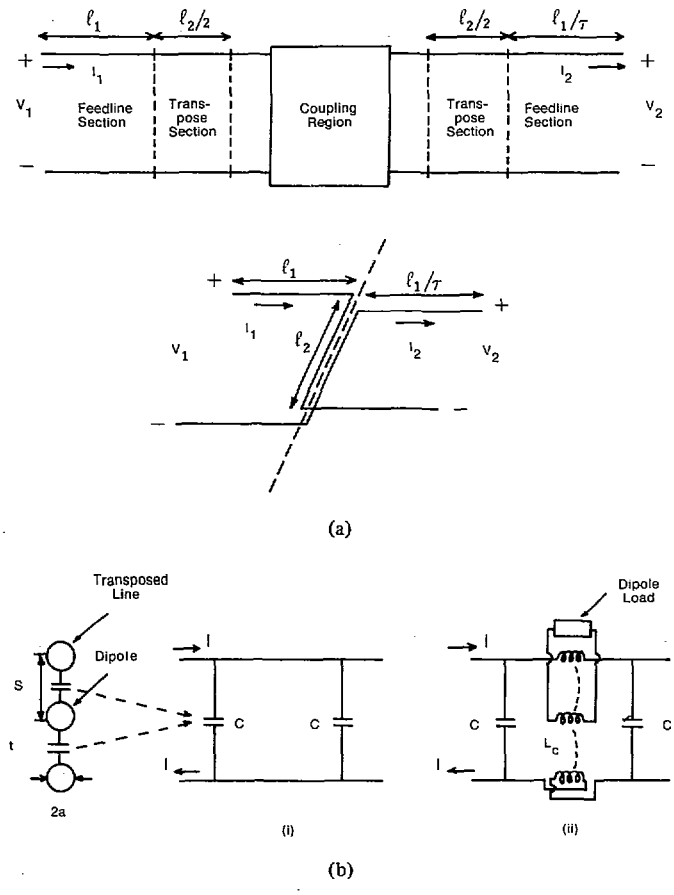

Fig. 2. (a) A typical cell of the loop-coupled LPDA showing the approximate network representation composed of transmission line sections and a coupling region. (b) The coupling region model (i) neglecting the dipole loading effect, and (ii) including the coupled dipole. Note that C is computed as two capacitors in series.

each transposition. Both the feedline and transposition sections are considered to be a single uniform balanced two-wire transmission line with the closer spaced transposition section represented by additional capacitance lumped at each end of the coupling region (Fig. 2(b)). This approximation has been used satisfactorily in the case of the flat conductor transposed transmission line [1] to calculate the phase velocity and to postulate the location of a transmission-line resonant region which could explain the frequency distribution of the experimentally observed anomalies. The dipole is coupled to the feeder through the inductance L_c given by Schelkunoff [2] and shown below in (1). Each of the lumped capacitors has a value given by (2).

$$L_c = \frac{\mu l_2}{2\pi}\left(\ln\frac{\lambda}{2\pi s} + 0.116 + Ci(\beta l_2) - \frac{\sin \beta l_2}{\beta l_2}\right) \tag{1}$$

$$C = \frac{l_2}{4}\,\frac{\pi\epsilon}{\cosh^{-1} s/_{2a}}. \tag{2}$$

Connecting several such cells in tandem yields the network in Fig. 3 where the boxed areas indicate sections of uniform two-wire transmission line whose length is equal to the transmission line distance between adjacent transposition centers. Writing the loop equations for the five-element array gives, after some manipulation:

$$-V_s(E^1 + G^1 Z_p^1)$$
$$= I_1(-F^1 - H^1 Z_p^1 - Z_s E^1 - Z_s G^1 Z_p^1) + I_3 Z_p^1$$
$$-V_s G^1 Z_p^1$$
$$= 2I_3 Z_p^1 - 2Z_c^1 I_{17} + I_4 Z_p^1 + I_1(-Z_s G^1 Z_p^1 - H^1 Z_p^1)$$
$$0 = I_4(-F^2 - H^2 Z_p^2 - E^2 Z_p^1 - G^2 Z_p^2 Z_p^1) + I_6 Z_p^2 + I_3 \cdot (-E^2 Z_p^1 - G^2 Z_p^1 Z_p^2)$$
$$0 = 2I_6 Z_p^2 - 2Z_c^2 I_{18} + I_7 Z_p^2 + I_4(-H^2 Z_p^2 - G^2 Z_p^2 Z_p^1) - I_3 G^2 Z_p^2 Z_p^1$$
$$0 = I_7(-F^3 - H^3 Z_p^3 - E^3 Z_p^2 - G^3 Z_p^3 Z_p^2) + I_9 Z_p^3 + I_6 \cdot (-E^3 Z_p^2 - G^3 Z_p^3 Z_p^2)$$
$$0 = 2I_9 Z_p^3 - 2Z_c^3 I_{19} + I_{10} Z_p^3 + I_7(-H^3 Z_p^3 - G^3 Z_p^3 Z_p^2) - I_6 G^3 Z_p^3 Z_p^2$$
$$0 = I_{10}(-F^4 - H^4 Z_p^4 - E^4 Z_p^3 - G^4 Z_p^4 Z_p^3) + I_{12} Z_p^4 + I_9 \cdot (-E^4 Z_p^3 - G^4 Z_p^4 Z_p^3)$$
$$0 = 2I_{12} Z_p^4 - 2Z_c^4 I_{20} + I_{13} Z_p^4 + I_{10}(-H^4 Z_p^4 - G^4 Z_p^4 Z_p^3) - I_9 G^4 Z_p^4 Z_p^3$$
$$0 = I_{13}(-F^5 - H^5 Z_p^5 - E^5 Z_p^4 - G^5 Z_p^4) + I_{15} Z_p^5 + I_{12} \cdot (-E^5 Z_p^4 - G^5 Z_p^5 Z_p^4)$$
$$0 = 2I_{15} Z_p^5 - 2Z_c^5 I_{21} + I_{16} Z_p^5 + I_{13}(-H^5 Z_p^5 - G^5 Z_p^5 Z_p^4) - I_{12} G^5 Z_p^5 Z_p^4$$
$$0 = I_{16}(Z_p^5 + Z_L') + I_{15} Z_p^5$$

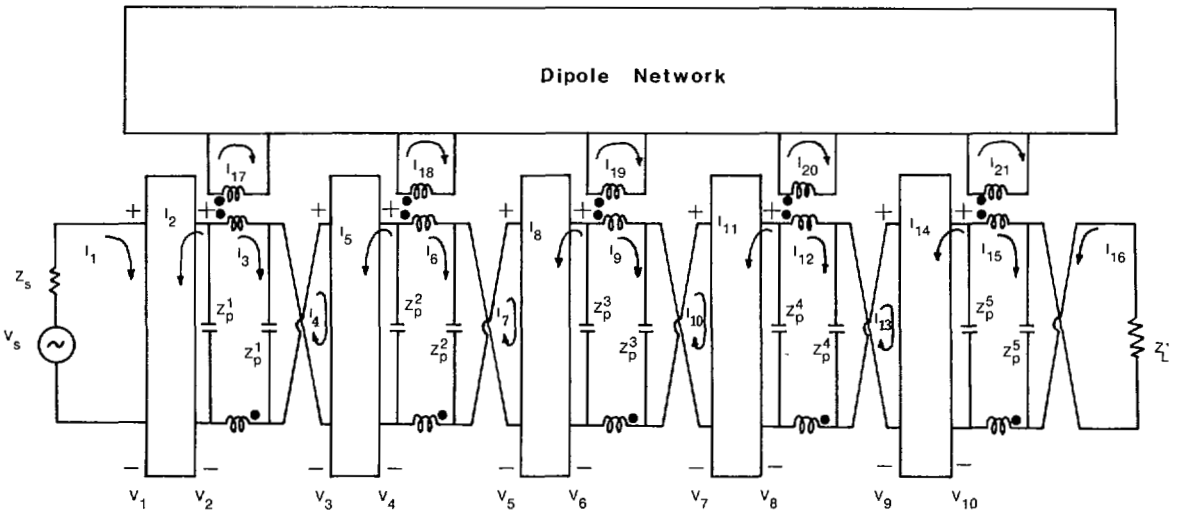

Fig. 3. Circuit model for a five-element loop-coupled LPDA. The boxes represent sections of uniform transmission line. The dipole network includes all element mutual coupling. Z_L' is the effective termination impedance as seen from the last transportation and includes the termination as well as the section of transmission line between the transposition and the termination.

$$
\begin{aligned}
0 &= I_{17}Z_A^{11} + I_{18}Z_A^{12} + I_{19}Z_A^{13} + I_{20}Z_A^{14} + I_{21}Z_A^{15} \\
&\quad - 2Z_c^1 I_3 \\
0 &= I_{18}Z_A^{22} + I_{17}Z_A^{21} + I_{19}Z_A^{23} + I_{20}Z_A^{24} + I_{21}Z_A^{25} \\
&\quad - 2Z_c^2 I_6 \\
0 &= I_{19}Z_A^{33} + I_{17}Z_A^{31} + I_{18}Z_A^{32} + I_{20}Z_A^{34} + I_{21}Z_A^{35} \\
&\quad - 2Z_c^3 I_9 \\
0 &= I_{20}Z_A^{44} + I_{17}Z_A^{41} + I_{18}Z_A^{42} + I_{19}Z_A^{43} + I_{21}Z_A^{45} \\
&\quad - 2Z_c^4 I_{12} \\
0 &= I_{21}Z_A^{55} + I_{17}Z_A^{51} + I_{18}Z_A^{52} + I_{19}Z_A^{53} + I_{20}Z_A^{54} \\
&\quad - 2Z_c^5 I_{15}
\end{aligned} \tag{3}
$$

where the two-port transmission parameters E, F, G, H are defined in Fig. 4, and Z_p and Z_c are the capacitive and inductive coupling impedances, respectively, given by

$$
\begin{aligned}
Z_p &= (j\omega C)^{-1} \\
Z_c &= j\omega L_c.
\end{aligned} \tag{4}
$$

Z_s and Z_L' are the source impedance and effective termination impedance (lumped load Z_L at the end of a section of transmission line) respectively, and Z_A^{mn} is the mutual impedance between the mth and nth dipoles calculated using an assumed single-sinusoid current distribution of the form $\sin \beta(h - |u|)$ where u is distance measured from the center. Superscripts refer to the cell numbering scheme commencing at the feedpoint. This system of equations was solved numerically by use of pivotal elimination.

III. RADIATION PATTERNS

The computed and measured swept-frequency front and back radiation patterns of two antennas (Fig. 5) show that their normal functioning is disrupted by distinct anomalies in both the frontlobe and backlobe. Comparison of these and other computed and measured patterns shows that anomaly frequencies are determined theoretically with less than 3 percent error. Experimental results consistently show a higher front-to-back ratio and somewhat shallower anomalies than do the theoretical curves; however, it must be noted that computations are based on average dimensions taken from the constructed models where mechanical tolerances were of the order of 15 percent for the parameter t and approximately 10 percent for σ and χ. In addition, the calculations assume lossless conductors in free space. Both measurements and theory show that the dips in the front pattern tend to be sharper than the corresponding peaks in the backlobe. Also, at higher frequencies there is a tendency for the backlobe peaks to broaden and to shift down in frequency with respect to the frontlobe dips.

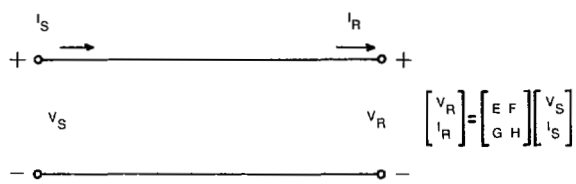

Fig. 4. Two-port transmission line network showing the voltage and current convention used in the definition of the transmission matrix parameters E, F, G, H.

The effect of the anomalies is especially noticeable with respect to the E-plane sidelobe levels (±90° from boresight). At frequencies other than the anomaly frequencies for the five-element antennas studied a typical sidelobe level of approximately 30–40 dB below the front lobe is possible over approximately a 50–80 MHz bandwidth. However, at the anomaly frequencies the sidelobe levels rise to as much as 5 dB below the frontlobe, accompanied by a 5–10 dB reduction in the front lobe. From the orientation of the feedline wires this side radiation must originate from the feedline.

IV. DIPOLE BASE CURRENT DISTRIBUTION

In normal operation at frequencies where anomalies do not occur the dipole current is concentrated in the elements located in front of the half-wavelength element (i.e., where the elements are shorter than $\lambda/2$). At the anomaly frequencies the dipole base currents are distributed in such a way that two or three dipoles carry large, nearly alternating-phase currents so that these

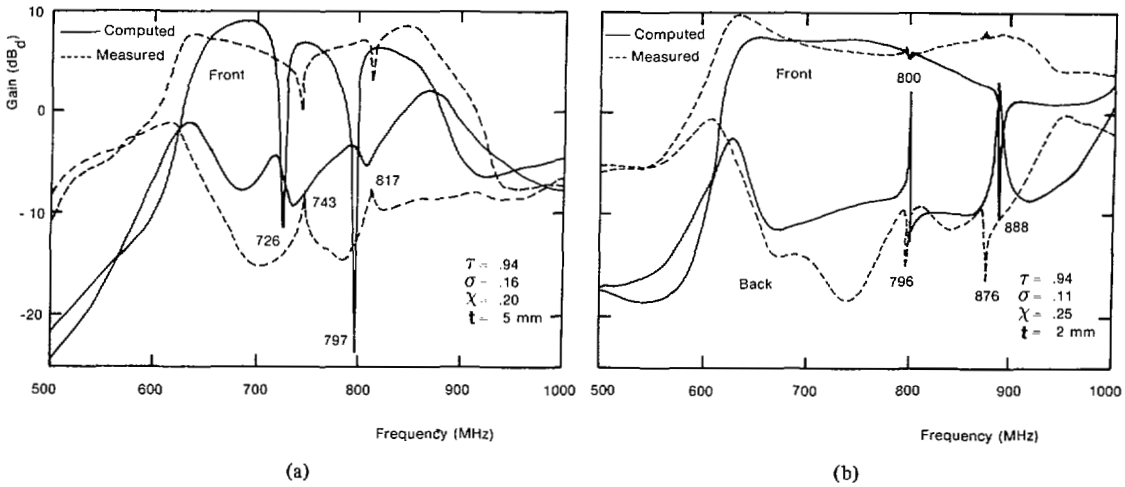

Fig. 5. Gain-frequency plots for two loop-coupled LPD arrays. Gain is given in decibels referred to a half-wavelength dipole. Numbers inset in the figures indicate the frequencies of the resonances in MHz. Each antenna has five elements. The longest dipole is a free-space half-wavelength at 700 MHz. All measured curves are continuous swept-frequency plots. (a) Short-circuit termination located 10 cm from center of longest transposition. (b) Short-circuit termination is located 12.6 cm from center of longest transposition.

dipoles appear to form a two or three-wire transmission-line-type of resonator. Similar anomalous dipole current distributions have been observed on the dispersionless LPDA [3] and the Yagi-Uda array [4]. Fig. 6 shows the magnitude and phase of the dipole base currents at the computed anomaly frequencies for the two antennas considered thus far. For a given antenna the anomaly peak currents generally decrease with increasing frequency. More compressed arrays (smaller σ) also tend to exhibit larger anomaly peak currents than do less compressed models. In addition the two antennas with $\sigma = 0.16$ and $\sigma = 0.11$, which were designed to match the transmission line phase velocity to near free space velocity at the half-wavelength dipole as recommended in [1], still exhibit strong resonances.

Examination of the location of the resonant "cell" (i.e., the group of dipoles carrying strong out-of-phase currents) on each of the antennas reveals that in each case the cell is located around the half-wavelength element at the frequency. As the frequency is increased this cell continues to move with the half-wavelength element until the half-wavelength frequency of the shortest element is reached. The anomalies are distributed log-periodically in frequency with a frequency ratio (defined as f_n/f_{n+1} where f_n and f_{n+1} are adjacent anomaly frequencies and $f_n < f_{n+1}$) slightly less than the scaling factor τ (the frequency ratios ranged from 0.90 to 0.93 for the antennas considered where $\tau = 0.94$).

V. PHASE CHARACTERISTICS

In [1] the phase characteristics of the uncoupled ($L_c = 0$) transposed transmission line were studied and can be used to "optimize" the loop-coupled LPDA design in the sense that the transmission line phase velocity (as sampled at the dipole coupling points) can be adjusted to match the free-space phase velocity near the location of the half-wavelength dipole. In other words, for a fixed transpose-to-dipole spacing t and feed ratio χ, there exists an "optimum" value of dipole spacing parameter σ_{opt}, such that the phase velocity is matched as described above.

Using the theoretical solutions for the transmission line currents or dipole base currents from the loop-coupled array model (complete with dipoles) one can plot the phase distribution curves shown in Fig. 7. These curves were drawn by calculating the phase shift per cell for each cell in the array at 2 MHz increments over the 500-1000 MHz frequency range and plotting representative values. These curves describe the coupling between the transmission line and the dipole array, as suggested in [1]; however, the present calculation includes the effects of dipole loading on the line which was not included in [1]. It should be noted that this phase distribution graph involves waves propagating in both the forward and backward (reflected) directions and should be similar to a dispersion curve only in the absence of standing waves. The curves in Fig. 7 do not include data from cells at anomaly frequencies. Shown in Fig. 7 is the dispersion curve for an infinitely long uniform array of dipole elements, obtained by interpolation of tabular data from Shen [5].

In Fig. 7 consider first the use of a matched resistive termination on the transmission line at the large end of the antenna. Below the $\lambda/2$ dipole line the transmission line curve nearly merges with the dipole curve, suggesting strong coupling from the forward wave on the line to the backward wave on the dipoles, the latter wave being the one which is eventually radiated off the small end of the antenna. In this region on the diagram the dipole curve is close to the dispersion curve for a wave on an infinitely long array. Above the $\lambda/2$ dipole line both the dipole curve and the transmission line curve indicate the propagation of a wave toward the resistive termination at the large end of the antenna.

Now consider in Fig. 7 the curve representing the phase of currents on the transmission line with a short circuit termination. At and immediately above the $\lambda/2$ dipole line this curve indicates approximate phase reversal between adjacent elements, the phase shift being closest to 180° for the cell between the half-wavelength dipole and the next longest dipole. Clearly these out-of-phase line currents could excite the transmission line type of resonance in the dipoles which are about a half-wavelength long (see Fig. 6). The remaining necessary condition for a parasitic resonance is the occurrence of a standing-wave current maximum near the half-wave element, a condition already noted by Oakes and Balmain [1]. Apparently, the "resonator" responsible for the gain anomalies comprises *both* the dipole pair (or triplet) slightly

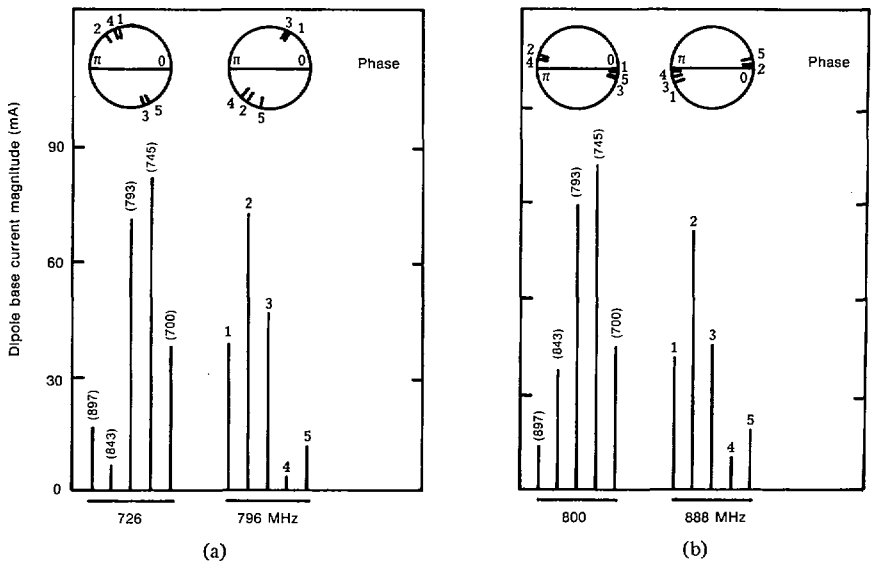

Fig. 6. Computed dipole base current distribution for two 5-element loop-coupled LPD arrays at anomaly frequencies. In all cases $\tau = 0.94$. Dipoles are numbered from the feed end. Numbers in brackets above dipole numbers indicate element $\lambda/2$ frequencies. Both arrays have short circuit termination. (a) $\sigma = 0.16$, $\chi = 0.20$, $t = 5$ mm, (b) $\sigma = 0.11$, $\chi = 0.25$, $t = 2$ mm.

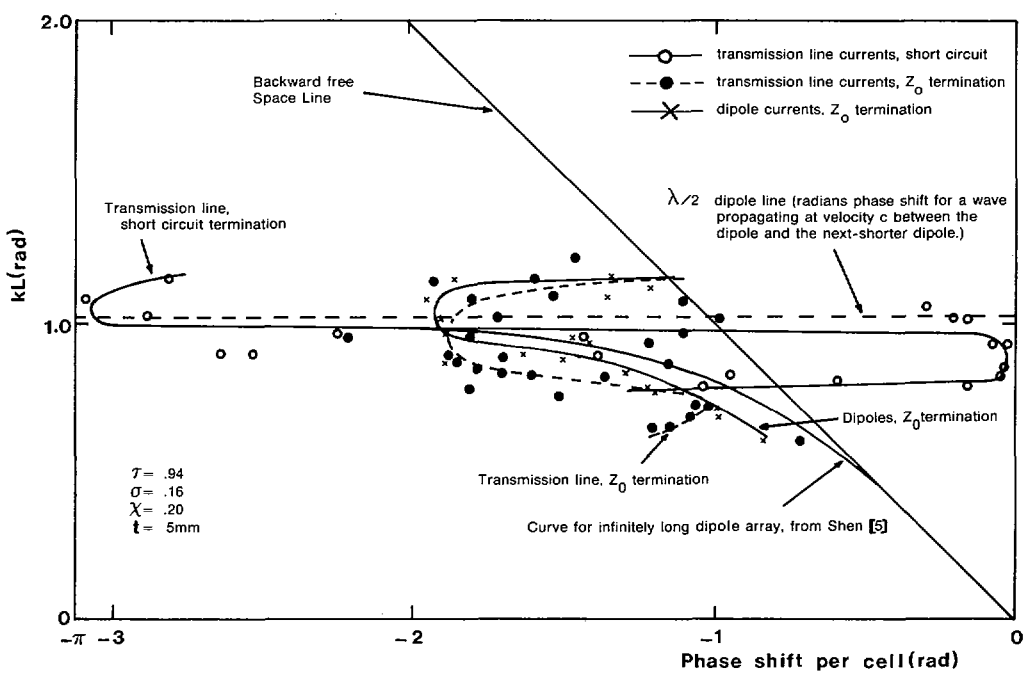

Fig. 7. Computed phase distribution curve for a five-element loop-coupled LPDA. Curves denoted —o— and --•-- are plotted from the phase characteristics of current along the transmission line for short circuit and Z_0 termination. Curve denoted by —×— plotted from phase characteristics of dipole base currents with Z_0 termination. L denotes the local cell length and $k = \omega/c$.

longer than $\lambda/2$ *and* the length of transmission line between them and the reactive large-end termination.

VI. TERMINATION EFFECT ON FAR FIELD

Both the computed and measured effects of termination impedance on the swept-frequency radiation characteristics indicate that the resonances are damped or eliminated through the use of a matched termination (Fig. 8), in confirmation of the corresponding experimental observation in [1]. For the antennas under consideration the average feedline characteristic impedance is approximately 400 Ω between transpositions. While it is a straightforward matter to specify a 400 Ω lumped load in the numerical program it is considerably more difficult physically to attach a load which has a constant resistive value over the entire frequency range of interest. For this purpose an electrically lossy dielectric material (Eccosorb VF) was used as a load by wrapping an approximately 2 cm wide strip around the transmission line

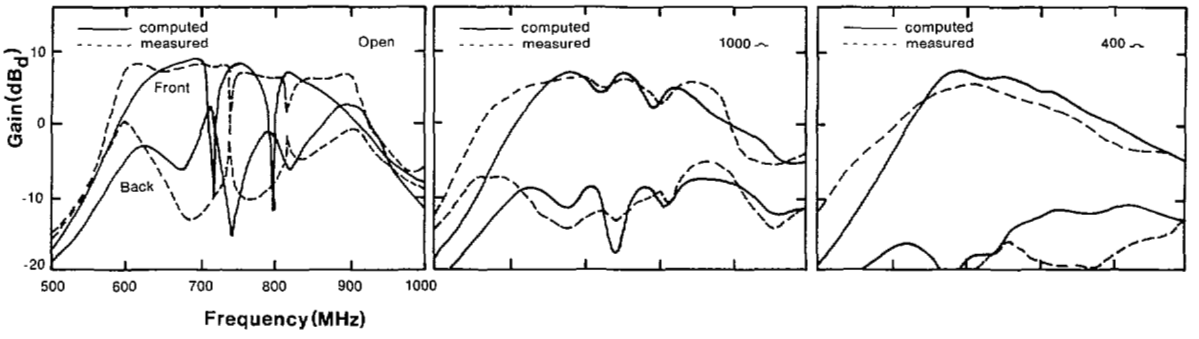

Fig. 8. Gain-frequency plots for five-element loop-coupled LPD arrays with $\tau = 0.94$, $\chi = 0.20$, $\sigma = 0.16$, $t = 5$ mm with (a) open circuit, (b) 1000 Ω, (c) 400 Ω termination. Termination is located 12.2 cm beyond center of longest transposition. Gain is in decibels referenced to λ/2 dipole.

terminals and measuring the approximate DC resistance between conductors through the lossy material.

VII. DEPENDENCE ON PARAMETERS χ, σ AND t

Twenty different five-element antennas were analyzed theoretically to study the effect of varying the parameters χ and σ while maintaining $t = 2.0$ mm and $\tau = 0.94$. In all cases for fixed χ the effect of increasing σ is to cause a downward anomaly frequency shift and an increase in the total number of anomalies in the 500-1000 MHz band.

The calculated dependence of bandwidth and front-to-back ratio upon χ and σ is shown in Fig. 9. The front-to-back ratio in each case was measured at the center of the useful passband B. A useful measure of the antenna bandwidth is the normalized bandwidth factor of the radiating region B_{ar}, defined by Carrel [7] as

$$B_{ar} = B_s/B \tag{5}$$

where B_s is the structure bandwidth (given by τ^{1-N} for an N-element array) and B is the so-called useful bandwidth here defined as the range of frequencies for which the front-to-back ratio exceeds a certain value. Mikhail [6] selected a value of 15 dB for his printed circuit antennas and Carrel's criteria [7] are considerably more complex, involving the element currents. In order to account for the observed antenna directivity in the present antennas (approximately 8 dB$_d$ for $\chi \cong 0.22$) it would seem reasonable to expect the radiating region to be at least three elements wide. The experimentally obtained values of B_{ar} versus χ for various criteria indicate that the 20 dB criterion yields an estimate of approximately three elements in the radiating region as compared with two for the 15 dB criterion. For all values of χ investigated the bandwidth parameter B_{ar} consistently shows a marked decrease from the estimates of Carrel and Mikhail except for certain cases when $\sigma > 0.18$. For these cases of larger σ the calculated bandwidth decreases rapidly with increasing σ, due primarily to the narrowing of the useful bandwidth B by the occurrence of very strong resonances which reduce the front-to-back ratio below the 15 dB criterion.

Fig. 9(b) shows that for the lightly coupled models ($\chi < 0.25$) the maximum front-to-back ratio occurs near $\sigma = 0.15$, whereas for tightly coupled antennas the best F/B performance will be obtained for $\sigma < 0.07$.

Fig. 10 presents the measured forward gain and front-to-back ratio for five experimental antennas as a function of χ with $\sigma = \sigma_{opt}$ where σ_{opt} is empirically related to χ by

$$\sigma_{opt} = -0.536\chi + b \tag{6}$$

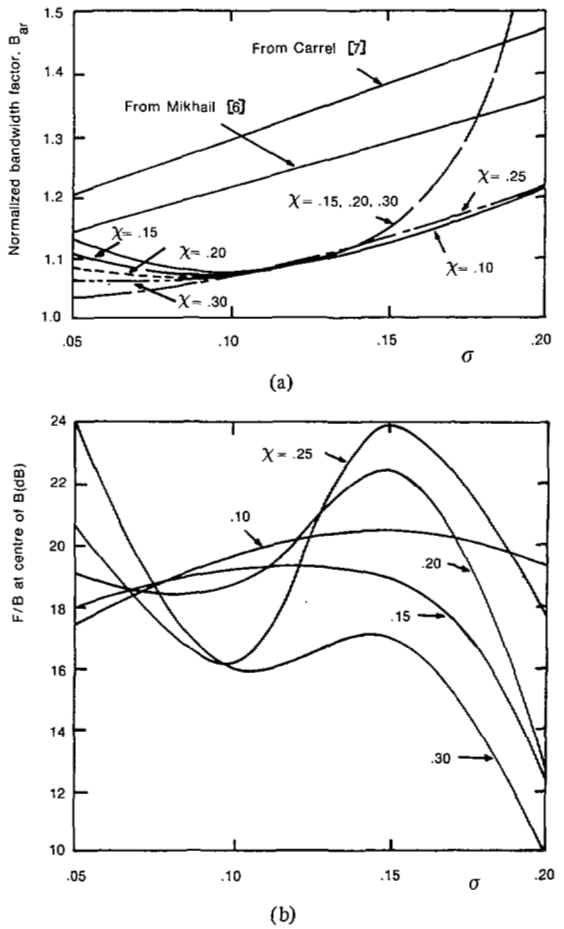

Fig. 9. (a) Calculated normalized bandwidth factor for five-element loop-coupled LPD antennas. Frequency limits are defined using 15 dB front-to-back criterion. $t = 2$ mm. (b) Calculated front-to-back ratio at center of operating band B for five-element loop-coupled LPD antennas, $t = 2$ mm.

where

$b = 0.227$ for $t = 1$ mm

$= 0.252$ for $t = 2$ mm

$= 0.268$ for $t = 5$ mm.

An optimum combination of gain and front-to-back ratio occurs at approximately $\chi = 0.25$ (with $\sigma = 0.11$, t = 2 mm). Comparison between Carrel's corrected gain figures [8] and the average computed gain figures in this study indicates that loop-coupled

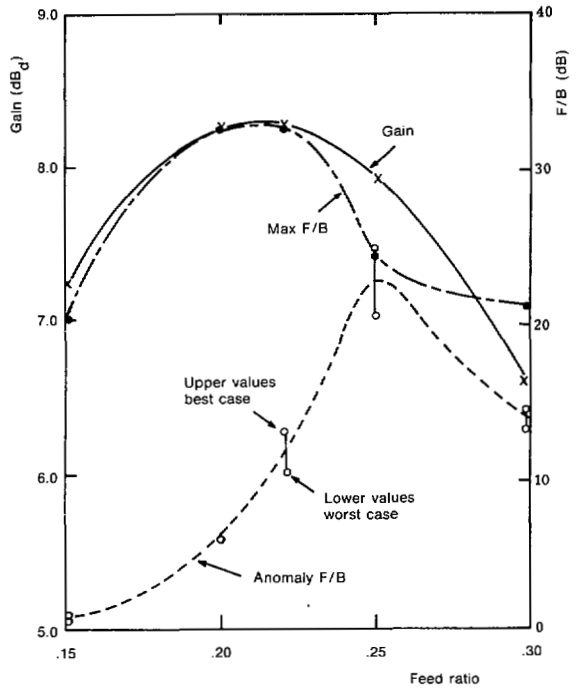

Fig. 10. Measured gain and front-to-back ratio for five experimental antennas, $N = 5$, $t = 2$ mm, $\tau = 0.94$, $\sigma = \sigma_{opt}$, short-circuit termination located 10.0 cm beyond center of longest transposition. For each of the five antennas the "best case" and "worst case" anomaly front-to-back were taken at the resonances where the front-to-back ratio was maximum and minimum, respectively.

antennas can be designed with gain performance comparable to that of their standard LPDA counterparts.

A theoretical study was undertaken to determine the dependence of antenna performance, particularly the resonance phenomenon, upon the spacing parameter t. Five-element antennas with $\chi = 0.25$ and $\sigma = 0.11$ were considered. The spacing parameter t was varied in nine steps from 1 to 5 mm in 0.5 mm increments and the far-field front and back radiation patterns were calculated.

The maximum front-to-back ratio shows a noticeable increase with t although the anomaly front-to-back ratios become much smaller for increasing t. An optimum tradeoff between maximum front-to-back ratio and anomaly front-to-back ratio appears to be for t approximately 1.5 to 2.0 mm.

Examination of the bandwidth characteristics of the nine antennas gives an average normalized bandwidth factor B_{ar} of 1.07 using the 15 dB front-to-back ratio criterion. A somewhat larger average value of 1.21 is obtained using the 20 dB front-to-back ratio criterion although this value is still smaller than the estimate of 1.23 using Mikhail's formula [6]. This increased bandwidth performance is consistent with measurements made on several experimental antennas.

The above design data were tested by application to a 15-element antenna having the same parameters as the one in Fig. 5(b). The antenna performed as expected in all respects except one: it had been designed for a 15 dB front-to-back ratio over a 2:1 bandwidth, but instead it exhibited a 20 dB front-to-back ratio over that bandwidth.

IX. INPUT IMPEDANCE

The swept frequency antenna input impedance has been calculated for several loop-coupled antennas; impedance measurements made at several frequencies (approximately 13 frequencies for each antenna) agree well with the calculated values. The most notable general feature of the impedance curves is the very rapid phase change often associated with the anomaly frequencies. For the antenna which exhibited the best anomaly control ($\sigma = 0.11$, $\chi = 0.25$) the operating bandwidth (approximately 700 to 760 MHz, corresponding to the maximum measured front-to-back ratio region) is characterized by an average real impedance of approximately 200 Ω and an average reactance of $-j50$ Ω. In the Smith chart impedance representation the anomaly at 800 MHz is readily identified as a sharp cusp; however, the anomaly at 888 MHz shows no such cusp. Using either the linear impedance graphs or the Smith chart presentation leads to the conclusion that terminal impedance is not a reliable indicator of anomalous performance, a point also cited by Oakes and Balmain [1].

X. CONCLUSION

A relatively simple theoretical model has been developed for analysis of the loop-coupled log-periodic dipole antenna. The model employs transmission-line theory to represent the feeder, mutual inductance to represent the feeder-to-dipole coupling mechanism, and a single sinusoid to represent the current distribution on each half of each dipole. Theoretical computations of antenna performance agree well enough with measurements to establish the utility of the theoretical model for design purposes. Design data are provided for optimizing gain and front-to-back ratio over a specified bandwidth. Both calculations and measurements show that the gain of a loop-coupled log-periodic dipole antenna is comparable to that of a standard LPDA and that the bandwidth is slightly greater.

One type of anomalous performance was studied in depth, namely the occurrence of narrow-band parasitic resonances which give rise to very high backlobe levels, levels which can exceed the frontlobe level if the feeder is too loosely coupled to the dipoles. In previous work these resonances had been associated with the existence of a high-level standing wave on the feeder between the location of the half-wave dipole and the location of a reactive large-end termination, a standing wave which always had a current maximum near the half-wave dipole under resonance conditions. In this work it is shown that the parasitic resonance is also associated with high-level out-of-phase currents on adjacent dipoles, for dipoles equal to a half-wavelength or slightly longer. In other words the high level resonance currents flow in both the feeder and the dipoles. Furthermore, it is confirmed both theoretically and experimentally that the parasitic resonance can be eliminated by the use of a matched resistive termination at the large end of the feeder.

A graph of computed phase shift per antenna cell versus cell length (analogous to a dispersion diagram) is shown to be useful in two ways. First it shows how a standing wave on the feeder can couple to a transmission-line mode on adjacent dipole elements, in order to produce a parasitic resonance. Second, it demonstrates in the normal radiating region the close coupling between feeder currents and dipole currents which is necessary for the antenna to function as an effective backward-wave radiator.

REFERENCES

[1] C. R. Oakes and K. G. Balmain, "Optimization of the loop-coupled log-periodic antenna," *IEEE Trans. Antennas Propagat.*, vol. AP-21, pp. 148–153, Mar. 1973.

[2] S. A. Schelkunoff and H. T. Friis, *Antennas: Theory and Practice*. New York: Wiley, 1962, pp. 236.

[3] J. M. Tranquilla and K. G. Balmain, "A study of TEM resonances on a class of parallel dipole arrays," in Proc. 1977 Antenna Applications Symp., Allerton Park, IL, Apr. 1977.

[4] ——, "Resonance phenomena on Yagi arrays," *Canadian Elect. Engi. J.*, vol. 6, no. 2, pp. 9–13, 1981.
[5] L. C. Shen, "Numerical analysis of wave propagation on a periodic linear array," *IEEE Trans. Antennas Propagat.*, vol. AP-19, pp. 289–292, Mar. 1971.
[6] S. W. Mikhail, "An experimental study of loop-coupled log-periodic dipole antennas," M.A.Sc. thesis, Univ. Toronto, Toronto, Canada, 1968.
K. G. Balmain and S. W. Mikhail, "Loop coupling to a periodic dipole array," *Electron. Lett.*, vol. 5, no. 11, pp. 228, 229, May 1969.
[7] R. L. Carrel, "Analysis and design of the log-periodic antenna," Tech. Rep. 52, antenna Lab., Univ. Illinois, Urbana, 1961.
——, "The design of log-periodic dipole antennas," *IRE Int. Conv. Rec.*, vol. 9, 1961, pp. 61–75.
[8] P. C. Butson and G. T. Thompson, "A note on the calculation of the gain of log-periodic dipole antennas," *IEEE Trans. Antennas Propagat.*, vol. AP-24, pp. 105–106, Jan. 1976.

James M. Tranquilla (S'68–M'73) was born in Millville, NB, Canada on May 1, 1948. He received the B.Sc.E. and M.Sc.E. degrees from the University of New Brunswick, Fredericton, NB, Canada, in 1971 and 1973, respectively, and the Ph.D. degree from the University of Toronto, Toronto, Canada, in 1979 in electrical engineering.

During the summers of 1970 and 1971 he was an Engineering Research Assistant with Defence Research Establishment Atlantic of DND, Canada. In 1977 he joined the Department of Electrical Engineering at the University of New Brunswick where he is currently an Associate Professor.

His research interests include broadband radiating systems, numerical techniques in electromagnetics and adaptive arrays.

Dr. Tranquilla is a member of Commission B of the International Union of Radio Science. He is a Registered Professional Engineer in the province of New Brunswick.

Keith G. Balmain (S'56–M'63) was born in London, ON, Canada on August 7, 1933. He received the B.A.Sc. degree in 1957 from the University of Toronto, Toronto, ON, Canada, in engineering physics, and the M.S. and Ph.D. degrees in 1959 and 1963 from the University of Illinois in Electrical Engineering.

For three years he was an Assistant Professor in Electrical Engineering at the University of Illinois, associated primarily with the Aeronomy Laboratory. In 1966 he joined the Department of Electrical Engineering at the University of Toronto where he is now a Professor. His research has focused on antennas in plasma, and also on broadband antennas with emphasis on anomalous performance and swept-frequency measurement techniques. His present research programs include radio wave scattering from power lines and high-rise buildings, EHF antennas, electrostatic charge accumulation and arc discharges on synchronous-orbit spacecraft, and participation in planning for the space shuttle waves-in-space-plasmas experiment.

Dr. Balmain was co-recipient of the IEEE Antennas and Propagation Society Best Paper of the Year award in 1970. He coauthored the second edition of *Electromagnetic Waves and Radiating Systems*. His IEEE activities include the following: Member of the Antenna Standards Committee and Chairman of the Subcommittee on Antennas in Physical Media (1967–76); Member, NRC Associate Committee on Radio Science and Canadian Chairman of the International Union of Radio Science Commission VI (1970–73); Associate Editor, *Radio Science* (1978–80).